Article

Aluminosilicate Surfaces as Promoters for Peptide Bond Formation: An Assessment of Bernal's Hypothesis by ab Initio Methods

Albert Rimola, Mariona Sodupe, and Piero Ugliengo

J. Am. Chem. Soc., **2007**, 129 (26), 8333-8344• DOI: 10.1021/ja070451k • Publication Date (Web): 07 June 2007

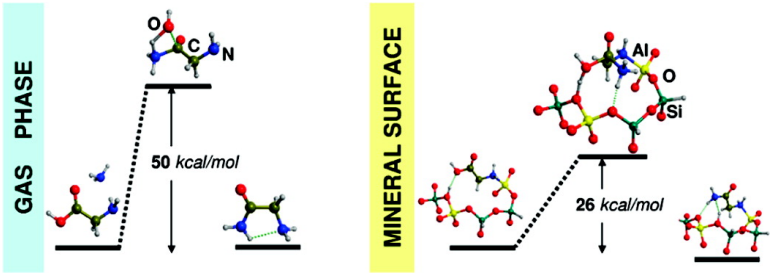

More About This Article

Additional resources and features associated with this article are available within the HTML version:

- Supporting Information
- Links to the 5 articles that cite this article, as of the time of this article download
- Access to high resolution figures
- Links to articles and content related to this article
- Copyright permission to reproduce figures and/or text from this article

View the Full Text HTML

J|A|C|S
ARTICLES
Published on Web 06/07/2007

Aluminosilicate Surfaces as Promoters for Peptide Bond Formation: An Assessment of Bernal's Hypothesis by ab Initio Methods

Albert Rimola,[†] Mariona Sodupe,*[,†] and Piero Ugliengo*[,‡]

Contribution from the Departament de Química, Universitat Autònoma de Barcelona, Bellaterra 08193, Spain, and Dipartimento di Chimica IFM, Università di Torino, Via P. Giuria 7, 10125 Torino and NIS-Nanostructured Interfaces and Surfaces - Centre of Excellence and INSTM (Materials Science and Technology) National Consortium, UdR Università di Torino, Italy

Received January 21, 2007; E-mail: piero.ugliengo@unito.it; mariona@klingon.uab.es

Abstract: The role in prebiotic chemistry that Brønsted and Lewis sites, both present at the surface of common aluminosilicates, may have played in favoring the peptide bond formation has been addressed by ab initio methods within a cluster approach. B3LYP/6-31+G(d,p) free energy potential energy surfaces have been fully characterized for the model reaction glycine + NH_3 → 2-NH_2 acetamide (mimicking the true 2 Gly → GlyGly one) occurring on (i) a Lewis site, (ii) a Brønsted site, and (iii) a combined action of Lewis/Brønsted sites. Compared to the gas-phase (gp) activation free energy of 50 kcal/mol, the Lewis site alone reduces the gp barrier to 41 kcal/mol, whereas the activation by the Brønsted site dramatically reduces the barrier to about 18 kcal/mol. Nevertheless, formation of the prereactant complex in this latter case will rarely occur, since water will easily displace the glycine molecule interacting with the Brønsted site. However, if a realistic feldspar surface with neighboring Brønsted and Lewis sites is considered, the proper prereactant complex is highly stabilized by a simultaneous interaction with the Lewis and the Brønsted sites, in such a way that the Lewis site strongly attaches the glycine molecule to the surface whereas the Brønsted site efficiently catalyzes the condensation reaction, showing that the interplay between Lewis/Brønsted sites is an important issue. The free energy barrier computed for the realistic feldspar surface model is 26 kcal/mol. The role of dispersive interactions on the free energy barrier and the stabilization of the final product, not accounted for by the B3LYP functional, have been estimated and shown to be substantial. Speculations about further elongation of the formed dipeptide have been put forward on the basis of the relatively strong interaction energy of the formed GlyGly dipeptide with the aluminosilicate surface.

Introduction

There are three main proposals about the prebiotic origin of molecules relevant for building up a living organism.[1−4] The earliest ones, based on the pioneering work of Miller,[5] Miller and Urey,[6] Lazcano and Miller,[7,8] and Oró,[9] were concerned with the idea of a chemoheterotrophic ("other nourishment") mechanism, that is, important molecular building blocks such as amino acids, purines/pyrimidines, and ribose were first synthesized at the earth's surface by reactive events in the primordial reducing atmosphere (CH_4, H_2O, NH_3, H_2) and then scavenged by what would become the first living organism. Along the same line of thought is a suggestion based on the work of Oró,[10] Allamandola et al.,[11] and Pizzarello,[12] envisaging the role of meteoritic bombardment in the first billion years of the earth's existence as a source of abiogenic important molecules (first synthesized in the interstellar clouds) of the same kind as those produced in Miller's experiment. The most recent proposal, however, springs from the discovery[13] of a complex ecosystem close to the hydrothermal "black smokers" in the deep ocean (more than 8000 feet down), by the Alvin submersible in 1977. The surprising evidence that life was possible without the support of photosynthetic processes,[14] stimulated Wachtershauer[15,16] to develop a chemoautotrophic ("self-nourishing") theory, in which the energy provided by the hydrothermal vents, coupled with the reducing power of iron

[†] Universitat Autònoma de Barcelona.
[‡] Università di Torino.

(1) Hazen, R. M. *Am. Mineral.* **2006**, *91*, 1715.
(2) Hazen, R. M. *Genesis: The Scientific Quest for Life's Origin*, 1st ed.; Joseph Henry Press: Washington, DC, 2005.
(3) Bada, J. L. *Earth Planet. Sci. Lett.* **2004**, *226*, 1.
(4) Rode, B. M. *Peptides* **1999**, *20*, 773.
(5) Miller, S. L. *Science* **1953**, *117*, 528.
(6) Miller, S. L.; Urey, H. C. *Science* **1959**, *130*, 245.
(7) Lazcano, A.; Miller, S. L. *J. Mol. Evol.* **1994**, *39*, 546.
(8) Lazcano, A.; Miller, S. L. *Cell* **1996**, *85*, 793.
(9) Oró, J. *Nature* **1961**, *191*, 1193.
(10) Oró, J. *Nature* **1961**, *190*, 389.
(11) Bernstein, M. P.; Sandford, S. A.; Allamandola, L. J.; Gillette, J. S.; Clemett, S. J.; Zare, R. N. *Science* **1999**, *283*, 1135.
(12) Pizzarello, S. *Origins Life Evol. Biosphere* **2004**, *34*, 25.
(13) Corliss, J. B.; Dymond, J.; Gordon, L. I.; Edmond, J. M.; von Herzen, R. P. *Science* **1979**, *203*, 1073.
(14) Baross, J. A.; Hoffman, S. E. *Origins Life Evol. Biosphere* **1985**, *15*, 327.
(15) Wachtershauer, G. *Microbiol. Rev.* **1988**, *52*, 452.
(16) Huber, C.; Wachtershauer, G. *Science* **1998**, *281*, 670.

10.1021/ja070451k CCC: $37.00

sulfide (abundant at the black smokers), was enough to synthesize important molecules which, in turn, gave rise to the first metabolic cycle.[17] Cleverly designed chemical reactions carried out by Hazen and co-workers[18] in test tubes simulating the same physicochemical conditions at the "black smokers" confirmed the power of hydrothermal organic synthesis. Continuing along the same scheme, an even more intriguing elaboration on the role of ocean hydrothermal vents on the origin of primordial cell membranes and metabolism has been proposed by Russell and Hall.[19]

Irrespective of the preferred path toward the synthesis of molecular building blocks, a rather critical step still remains to be understood: how do amino acids or purines and pyrimidines find their way toward polypeptides and nucleic acids? Even focusing only on the simplest amino acids, the above point is crucial for two main reasons: (i) the reaction needed for the synthesis of polypeptides is, in all cases, a condensation with water elimination, envisaging a rather high kinetic barrier (calculations carried out in our laboratory for a gas-phase condensation of two glycines at B3LYP/6-31+G(d,p) give a free energy barrier around 50 kcal/mol) and (ii) condensation reactions occurring in highly diluted water solutions are thermodynamically disfavored. British biophysicist Bernal[20] suggested, as early as 1953, that the internal surface of clay minerals may have played a key role in helping the reaction to occur by (i) providing adsorption sites that can immobilize, protect from hydration, and concentrate the amino acids from the dilute soup and (ii) lowering the activation barrier of the condensation reaction due to the catalytic effect of the surface active sites. These early speculative suggestions have been expanded by many groups by a series of well-designed experiments on a variety of inorganic materials, by no means limited to the suggested clay family.[21−25] Despite the great deal of experimental work upon the polymerization of simple amino acids by silica,[26−32] clays,[21,23,29,30,33,34] and aluminas,[26,28−30,35−38] very little is known about the mechanistic steps at the surface of these materials that are crucial for the activation of the peptide bond. Nevertheless, some mechanisms have been suggested in the past to interpret the experimental evidence of the formation of small oligopeptides, albeit at the level of very simple schemes by Zamaraev et al. for adsorption of glycine on zeolites and kaolinite,[32] by Bujdàk and Rode for hectorite,[30] silica, alumina,[29,36] or clays,[33] and by Basiuk et al. for silica and alumina.[26] Basically, all the mentioned experimental studies dealt with the detection of oligopeptides in the reaction products by means of standard analytical techniques. Unfortunately, only a few studies[26,31] adopted spectroscopic techniques to characterize the intimate changes of the molecular structure of the adsorbed amino acids, as well as to propose a well-grounded mechanism toward their polymerization.

On the theoretical side, a review article summarizing the modeling of active sites at the clay mineral surfaces has recently appeared,[39] whereas interesting Car−Parrinello dynamical simulations of glycine adsorbed on both nondefective and defective pyrite surfaces have also been reported.[40−42] More specifically, the catalytic activity of Lewis and Brønsted sites at aluminosilicate surfaces on the peptide bond formation has been studied by ab initio methods by Aquino et al.[43] by using very small cluster models. More recently, AlF_3 and HF have been adopted by some of us as generic models of Lewis and Brønsted acidity to study the activation of the simplified reaction $HCOOH + NH_3 \rightarrow NH_2-COH + H_2O$, and it was found that the interplay between the two acidic centers was crucial for lowering the kinetic barrier toward the peptide bond formation.[44] The possible catalytic role of pure silica as a peptide bond promoter, as suggested by Basiuk et al.[26] and Meng et al.,[31] has also been recently studied by ab initio methods by some of us and shown to exclude relevant activation of the peptide bond formation because of the presence of the surface mixed anydride Si−O−C═O−R bond.[45] To our knowledge, the catalytic role of true Lewis/Brønsted sites, both alone or co-present on a aluminosilicate surface on the peptide bond formation, has never been addressed with a realistic representation of the mineral surface.

The purpose of the present work is to investigate, by a fully ab initio approach, the above model reaction catalyzed by active sites present at the surface of aluminosilicate minerals. Following a suggestion by Smith[46] about the catalytic role of feldspars as the most abundant minerals in the earth's crust, we used anorthite and sanidine (most common feldspar constituents) as reference minerals. These materials envisage a silica-based framework in which Ca^{2+} or K^+ is present as charge-balancing cations for the Al substitution. The hydration of the surfaces of these materials, together with fluctuating thermal conditions, will allow for the exchange of some of the cations by protons, resulting in surfaces rich in Lewis and Brønsted sites, as happens for the preparation of acidic zeolites used as cracking catalysts. Figure 1 shows a ball-and-stick model of a possible H-exchanged sanidine surface: terminal silanols (Si−OH) and Brønsted and Lewis sites with a coordinated water are all present as active surface sites. As seen in Figure 1, Lewis and Brønsted sites can also be rather proximal in space, so that their interplay

(17) Wachtershauer, G. *Proc. Natl. Acad. Sci. U.S.A.* **1990**, *87*, 200.
(18) Cody, G. D.; Boctor, N. Z.; Filley, T. R.; Hazen, R. M.; Scott, J. H.; Sharma, A.; Yoder, H. S., Jr. *Science* **2000**, *289*, 1339.
(19) Russell, M. J.; Hall, A. J. *J. Geophys. Soc. London* **1997**, *154*, 377.
(20) Bernal, J. D. *The Physical Basis of Life*; Routledge and Kegan Paul: London, 1951.
(21) Lahav, N.; White, D. H.; Chang, S. *Science* **1978**, *201*, 67.
(22) Orgel, L. E. *Origins Life Evol. Biosphere* **1998**, *28*, 227.
(23) Rao, M.; Odom, D. G.; Orò, J. *J. Mol. Evol.* **1980**, *15*, 317.
(24) Hazen, R. M. *Sci. Am.* **2001**, *April*, 76.
(25) Pitsch, S.; Eschenmoser, A.; Gedulin, B.; Hui, S.; Arrhenius, G. *Origins Life Evol. Biosphere* **1995**, *25*, 297.
(26) Basiuk, V. A.; Gromovoy, T. Y.; Golovaty, V. G.; Glukhoy, A. M. *Origins Life Evol. Biosphere* **1990−1991**, *20*, 483.
(27) Basiuk, V. A. Adsorption of biomolecules at silica. In *Encyclopedia of Surface and Colloid Science*; Hubbard, A. T., Ed.; Marcel Dekker: New York, 2002; p 277.
(28) Bujdàk, J.; Rode, B. M. *React. Kinet. Catal. Lett.* **1997**, *62*, 281.
(29) Bujdàk, J.; Rode, B. M. *J. Mol. Evol.* **1997**, *45*, 457.
(30) Bujdàk, J.; Rode, B. M. *Origins Life Evol. Biosphere* **1999**, *29*, 451.
(31) Meng, M.; Stievano, L.; Lambert, J. F. *Langmuir* **2004**, *20*, 914.
(32) Zamaraev, K. I.; Romannikov, V. N.; Salganik, R. I.; Wlassoff, W. A.; Khramtsov, V. V. *Origins Life Evol. Biosphere* **1997**, *27*, 325.
(33) Bujdàk, J.; Rode, B. M. *J. Mol. Catal. A: Chem.* **1999**, *144*, 129.
(34) Collins, J. R.; Loew, G. H.; Luke, B. T.; White, D. H. *Origins Life Evol. Biosphere* **1988**, *18*, 107.
(35) Basiuk, V. A.; Sainz-Rojas, J. *Adv. Space Res.* **2001**, *27*, 225.
(36) Bujdàk, J.; Rode, B. M. *Amino Acids* **2001**, *21*, 281.
(37) Bujdàk, J.; Rode, B. M. *J. Inorg. Biochem.* **2002**, *90*, 1.
(38) Bujdàk, J.; Rode, B. M. *Catal. Lett.* **2003**, *91*, 149.
(39) Boulet, P.; Greenwell, H. C.; Stackhouse, S.; Coveney, P. V. *J. Mol. Struct.: THEOCHEM* **2006**, *762*, 33.
(40) Boehme, C.; Marx, D. *J. Am. Chem. Soc.* **2003**, *125*, 13362.
(41) Nair, N. N.; Schreiner, E.; Marx, D. *J. Am. Chem. Soc.* **2006**, *128*, 13815.
(42) Pollet, R.; Boehme, C.; Marx, D. *Origins Life Evol. Biosphere* **2006**, *36*, 363.
(43) Aquino, A. J. A.; Tunega, D.; Gerzabek, M. H.; Lischka, H. *J. Phys. Chem. B* **2004**, *108*, 10120.
(44) Rimola, A.; Tosoni, S.; Sodupe, M.; Ugliengo, P. *Chem. Phys. Lett.* **2005**, *408*, 295.
(45) Rimola, A.; Tosoni, S.; Sodupe, M.; Ugliengo, P. *ChemPhysChem* **2006**, *7*, 157.
(46) Smith, J. V. *Proc. Natl. Acad. Sci. U.S.A.* **1998**, *95*, 3370.

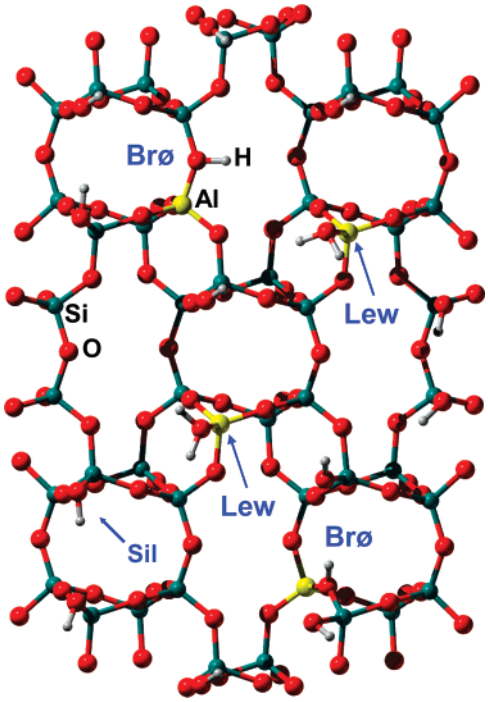

Figure 1. Top view of the bare H-exchanged feldspar sanidine surface. Lew (Lewis), Brø (Brønsted), and Sil (Silanol) active sites are shown. The Lew site coordinates a water molecule in virtue of its strong acidity.

in the adsorption and catalysis may be an important issue. A fully periodic ab initio calculation of the model condensation reaction (vide supra) catalyzed by the H-exchanged sanidine surface is, at present, undoable, considering that full characterization of transition-state structures is also needed as well as the computation of the free energies. To better understand the separate role of the Brønsted and Lewis sites, finite clusters based on hydridosilasesquioxanes cages (vide infra) have been designed, which minimize the number of terminal (and spurious) atoms and are particularly easy to optimize. The sanidine surface was used as a source for cutting out finite clusters mimicking the co-presence of Lewis and Brønsted sites to understand their possible interplay in the peptide bond activation. The same sanidine cluster will also be used to establish the fate of the newly formed dipeptide in terms of its likelihood of remaining adsorbed at the surface and becoming elongated by further glycine addition, in the same line suggested by Orgel[22] in his polymerization on the rocks model.

It should be stressed that the problem studied here is not limited to the field of origin of life or prebiotic chemistry. The interest in silica-based surfaces of which aluminosilicates identify a broad family of common materials stems also from the emerging field devoted to understanding the interaction of biomolecules with inorganic materials, as in the case of proteins on solid surfaces,[47] the biomimetic intergrowth of silica and polypeptides,[48] and the self-assembly of peptides on mica substrates.[49] Understanding the microscopic mechanisms responsible for the condensation of amino acids at the mineral surfaces in primitive earth will also be useful to clarify the basic interactions of today's proteins with inorganic materials of natural or synthetic origin.

(47) Gray, J. J. *Curr. Opin. Struct. Biol.* **2004**, *14*, 110.
(48) Bellomo, E. G.; Deming, T. J. *J. Am. Chem. Soc.* **2006**, *128*, 2276.

Computational Details

All calculations were performed using the GAUSSIAN03 program.[50] The level of theory used depended on the cluster considered to model the surface. For isolated Lewis and Brønsted sites, the cluster models adopted were small enough (vide infra) that full optimization of the system using the hybrid B3LYP density functional approach[51,52] with the 6-31+G(d,p) standard Pople's basis set was feasible. However, the cluster adopted to model a surface that contained both Lewis and Brønsted sites (vide infra) was too large to efficiently explore the potential energy surface (PES) at the B3LYP/6-31+G(d,p) level. Therefore, in this case, all structures were optimized using the ONIOM2 strategy combining the B3LYP/6-31+G(d,p) method, for the high-level zone, with the MNDO Hamiltonian, for the real system.[53] Once the stationary points were located, the energy was re-evaluated by performing single point calculations at the B3LYP/6-31+G(d,p) level on the optimum ONIOM2 geometries (hereafter referred to as B2 energies). The adopted ONIOM2[B3LYP/6-31+G(d,p):MNDO] combination proved to be a good compromise between accuracy and speed of calculation for silica[54] and zeolite modeling studies.[55] Furthermore, the reliability of B3LYP/6-31+G(d,p) to describe the PES of the considered reactions was recently validated[44] by comparing the B3LYP/6-31+G(d,p) results with the CCSD(T)/6-311++G(2d,2p) ones, and the results showed that the activation and reaction energies are underestimated by the DFT method by about 3 kcal/mol.

Because the adopted methodology did not take into account dispersive forces due to fluctuating instantaneous dipoles, a rather simple strategy was adopted here, to at least partially take them into account for the processes occurring on the sanidine-derived cluster. The DFT+D method recently proposed by Grimme has been adopted[56] and has been proved to be very effective for a number of cases where dispersive interactions are expected to be relevant.[56,57] The dispersive correction to the B2 energy (hereafter referred as B2+D) was carried out, in a posteriori fashion, by implementing the Grimme routine in the MOLDRAW program[58] and adding the resulting contribution to the B2 total energy.

All structures were characterized by the analytical calculation of the harmonic frequencies as minima (reactants and products) and saddle points (transition structures). In some cases, intrinsic reaction coordinate calculations were also carried out to confirm that the localized transition structure connects the desired reactants and products. Free energy profiles were derived by using the standard rigid rotor/harmonic oscillator formulas on the corresponding electronic energy values.

Manipulation, visualization, and preparation of structures were obtained with the MOLDRAW program,[58] whereas graphical rendering of the pictures was done by the POVRAY program using the input files prepared by MOLDRAW.

Results and Discussion

The condensation between two glycine molecules takes place when the nucleophilic nitrogen atom belonging to one amino acid attacks the carboxyl carbon atom of the second amino acid. This step is then followed by the elimination of one water

(49) Whitehouse, C.; Fang, J.; Aggeli, A.; Bell, M.; Brydson, R.; Fishwick, C. W. G.; Henderson, J. R.; Knobler, C. M.; Owens, R. W.; Thomson, N. H.; Smith, D. A.; Boden, N. *Angew. Chem., Int. Ed.* **2005**, *44*, 1965.
(50) Frisch, M. J.; et al. *Gaussian 03*, revision C.02; Gaussian, Inc.: Wallingford, CT, 2004.
(51) Becke, A. D. *J. Chem. Phys.* **1993**, *98*, 5648.
(52) Lee, C.; Yang, W.; Parr, R. G. *Phys. Rev. B* **1988**, *37*, 785.
(53) Maseras, F.; Morokuma, K. *J. Comput. Chem.* **1995**, *16*, 1170.
(54) Roggero, I.; Civalleri, B.; Ugliengo, P. *Chem. Phys. Lett.* **2001**, *341*, 625.
(55) Solans-Monfort, X.; Sodupe, M.; Branchadell, V.; Sauer, J.; Orlando, R.; Ugliengo, P. *J. Phys. Chem. B* **2005**, *109*, 3539.
(56) Grimme, S. *J. Comput. Chem.* **2006**, *27*, 1787.
(57) Antony, J.; Grimme, S. *Phys. Chem. Chem. Phys.* **2006**, *8*, 5287.
(58) Ugliengo, P. *MOLDRAW: A molecular graphics program to display and manipulate molecular structures*, version 2.0; University of Torino: Torino, Italy, 2006. http://www.moldraw.unito.it.

Scheme 1

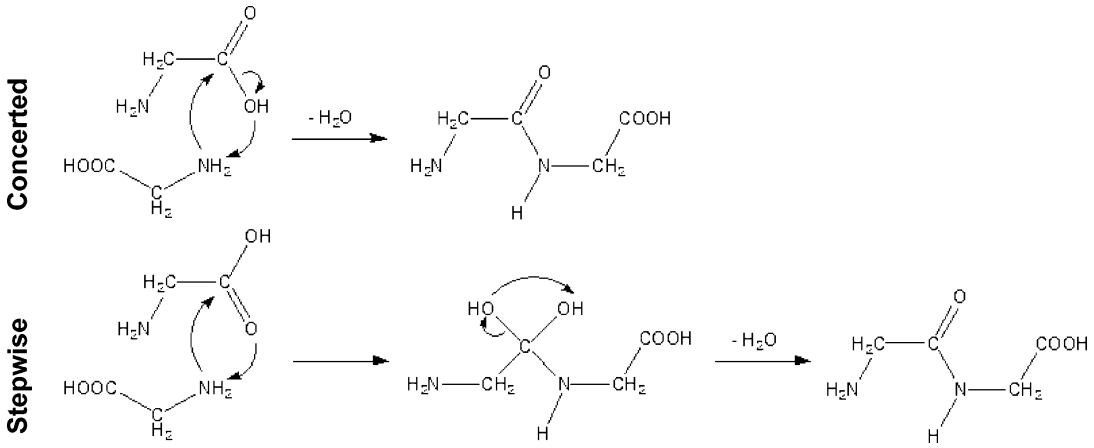

molecule and the formation of the HN−C═O peptide bond. It is well known that this reaction can proceed either by a concerted or by a stepwise mechanism.[59] In the former, during the nucleophilic attack, one hydrogen atom of the NH_2 group of the first glycine is transferred to the OH group of the second glycine, with subsequent release of water. In the latter, water is not released in a concerted way, because the proton transfer occurs toward the carbonyl oxygen instead of the hydroxyl group. In this way, a stable diolic intermediate is first formed which, in a second step, proceeds to an internal elimination of the water molecule (Scheme 1).

In the present work, considering the rather large number of calculations to be performed, the reaction between two glycine molecules on the Lewis or Brønsted sites has been simplified by considering one glycine (G) molecule and ammonia (NH_3) as reactants, as already anticipated in the Introduction. The condensation reaction gives rise to 2-amino acetamide ($H_2NCH_2C(O)NH_2$), a product simpler than the diglycine, which, however, already sports the HN−C═O bond, while reducing the conformational variability. The use of NH_3 to replace glycine has already been proposed in a seminal computational paper by Jensen,[60] in which it was shown that the G + NH_3 reaction has an energy barrier and a reaction energy that are very close to the full reaction envisaging two glycine molecules. The same has been found to hold true also with the present level of theory, and the results are available as Supporting Information.

Results are organized in the following way. First, we address the peptide bond formation on an isolated Lewis site; previously, we explored the possible adducts formed between the surface site and glycine molecule, in competition with adsorbed water. The same procedure is followed when considering the reaction on an isolated Brønsted site. As a last and more complicated step, the peptide bond formation using the sanidine-derived model that envisages the interplay between Lewis/Brønsted pair is illustrated. Finally, the possible role that mineral surfaces could have played in prebiotic conditions in the oligomerization of peptides is also discussed.

Lewis Site. The surface Lewis site is represented by a three-coordinated aluminum at the top of a $H_8Si_8O_{12}$ cluster belonging to the hydridosilasesquioxane family, which has been previously suggested as a convenient model to mimic silica-based active sites as isolated surface silanols.[61,62] Considering that the mineral surface is usually hydrated, an extra water molecule is coordinated to the Al atom to mimic the presence of water in the reaction medium (see ZL−H_2O in Figure 2). Similar clusters have recently been successfully used by some of us to mimic Lewis and Brønsted (vide infra) sites in β-zeolite and H-ZSM5 zeolites interacting with a variety of probe molecules and showed good agreement with the calorimetric measurements of the heats of adsorption.[63−66]

The very first stage is to displace the water molecule adsorbed on the Lewis site by glycine itself. Figure 2 also shows the possible adducts formed between glycine and the Lewis site. As summarized in Table 1, glycine adsorbs more tightly than water for all considered cases (Table 1, Lewis section). The most stable structure, ZL−G1, shows a direct Al−O bond with the carbonyl oxygen, while the OH group is involved in a strong hydrogen bond with the oxygen atom of the aluminosilicate surface, directly bound to the Al atom. In ZL−G2 (1 kcal/mol higher in free energy than ZL−G1), the NH_2 group is bound to the Al atom, with glycine keeping its most stable gas-phase conformation. Whereas both ZL−G1 and ZL−G2 envisage neutral glycine, in the ZL−G3 complex the zwitterionic form interacts with the Al of the surface through one of the carboxylate oxygens. This structure lies 4.7 kcal/mol higher in free energy than ZL−G1, showing that entropic effects disfavor the zwitterionic form (the electronic energy instability is only about 1.4 kcal/mol). For all considered structures, the Al atom adopts a tetrahedral coordination when interacting with glycine and any attempt to obtain a minimum structure of glycine interacting simultaneously through the C═O and NH_2 groups, as found for many metal cations,[67] failed and all collapsed to ZL−G1.

Figure 3 shows the B3LYP/6-31+G(d,p) free energy profiles of the concerted reactions for the different cases described above. The relative free energies of the different stationary points have been computed taking ZL−G1 + NH_3 as an asymptote. Only

(59) Jensen, J. H.; Baldridge, K. K.; Gordon, M. S. *J. Phys. Chem.* **1992**, *96*, 8340.
(60) Jensen, F. *J. Am. Chem. Soc.* **1992**, *114*, 9533.
(61) Sauer, J.; Hill, J. *Chem. Phys. Lett.* **1994**, *218*, 333.
(62) Civalleri, B.; Garrone, E.; Ugliengo, P. *Langmuir* **1999**, *15*, 5829.
(63) Bolis, V.; Barbaglia, A.; Broyer, M.; Busco, C.; Civalleri, B.; Ugliengo, P. *Origins Life Evol. Biosphere* **2004**, *34*, 69.
(64) Busco, C.; Barbaglia, A.; Broyer, M.; Bolis, V.; Foddanu, G. M.; Ugliengo, P. *Thermochim. Acta* **2004**, *418*, 3.
(65) Bolis, V.; Broyer, M.; Barbaglia, A.; Busco, C.; Foddanu, G. M.; Ugliengo, P. *J. Mol. Catal. A: Chem.* **2003**, *204*, 561.
(66) Bolis, V.; Busco, C.; Ugliengo, P. *J. Phys. Chem. B* **2006**, *110*, 14849.
(67) Bertran, J.; Rodriguez-Santiago, L.; Sodupe, M. *J. Phys. Chem. B* **1999**, *103*, 2310.

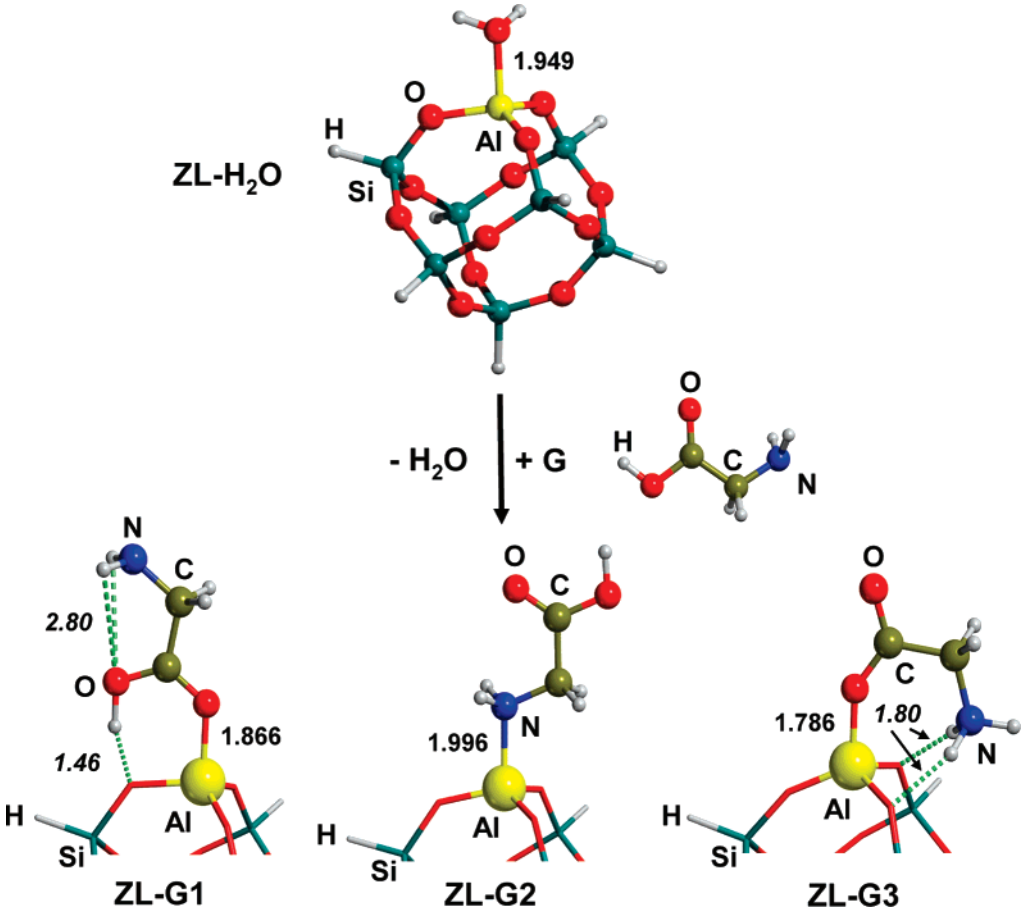

Figure 2. B3LYP/6-31+G(d,p)-optimized geometries of the cluster adopted to model the isolated Lewis site interacting with water (ZL−H_2O) and of the structures found when adsorbed water is replaced by glycine (ZL−G1, ZL−G2, and ZL−G3). Bond distances are in angstroms.

Table 1. Electronic Energy (ΔE_{displ}) and Free Energy (ΔG_{displ}) of the Water Displacement Reactions for the Lewis ZL−H_2O + G → ZL−G + H_2O, Brønsted ZB−H_2O + G → ZB−G + H_2O, and Lewis/Brønsted ZLB−H_2O + G → ZLB−G + H_2O Cases, Respectively[a]

	ΔE_{displ}	ΔG_{displ}	ΔE_{rel}	ΔG_{rel}
Lewis				
ZL−G1	−11.9	−10.1	0.0	0.0
ZL−G2	−10.8	−9.2	1.1	0.9
ZL−G3	−10.5	−5.4	1.4	4.7
Brønsted				
ZB−G1	−4.3	−5.4	0.0	0.0
ZB−G2	−3.5	−4.4	0.8	1.0
ZB−G3	7.8	4.3	12.1	9.7
Lewis/Brønsted				
ZLB−G1	(−12.6)	(−9.4)	(0.0)	(0.0)
	[−15.9]	[−12.7]	[0.0]	[0.0]
ZLB−G2	(−8.2)	(−5.3)	(4.4)	(4.1)
	[−11.7]	[−8.8]	[4.2]	[3.9]

[a] ΔE_{rel} and ΔG_{rel} are the corresponding relative energies with respect to the most stable structure (ZL−G1, ZB−G1, and ZLB−G1, respectively) computed for ZL, ZB, and ZLB sites. Bare numbers at B1 = B3LYP/6-31+G(d,p), numbers in parentheses at B2 = B1//ONIOM[B3LYP/6-31+G(d,p):MNDO], and numbers in square brackets at B2+D (Grimme's dispersion[56] included). Data are in kilocalories per mole.

the most relevant structures, along the energy profiles, have been reported in the figure (more details are available in the Supporting Information). Table 2 shows the energy barriers and the reaction energies for the computed processes (Table 2, Lewis section). Focusing on the energy barriers, results indicate that glycine is only activated by the surface as a ZL−G1 complex, with the energy barrier lowered by about 11 kcal/mol compared to the gas-phase reaction value. In contrast, when the reaction takes place via ZL−G2 and ZL−G3 complexes, the Lewis site does not show any catalytic activity, and the computed barriers are very similar to that of the gas-phase reaction. It is noteworthy that, for the ZL−G1 complex, the first reaction intermediate shows a rather short C−N distance (1.621 Å; see Supporting Information) as a consequence of the strong nucleophilic activation by the Al coordination through the oxygen atom of the O═C group, which becomes elongated by almost 0.05 Å. A similar behavior was reported for formic acid coordinated to AlF_3, as a model cluster of the Lewis acid.[44]

In the above reactions, the water molecule displaced by the incoming glycine from the starting ZL−H_2O complex is excluded from the reactive process. However, the relevance of water molecules as potential proton transfer helpers is well known,[68−71] and their role in the rate-determining step in which a proton transfers from the NH_3 molecule to the hydroxyl oxygen of glycine has been studied. For the sake of brevity, the role of water has been studied only on the ZL−G1 path, the latter being the one with the lowest kinetic barrier. As shown in Figure 2, the free energy barrier (27.2 kcal/mol) is dramatically reduced compared to the mechanism without water intervention (40.7 kcal/mol). This indicates the importance of

(68) Gauld, J. W.; Audier, H.; Fossey, J.; Radom, L. *J. Am. Chem. Soc.* **1996**, *118*, 6299.
(69) Chalk, A. J.; Radom, L. *J. Am. Chem. Soc.* **1997**, *119*, 7573.
(70) Gauld, J. W.; Radom, L. *J. Am. Chem. Soc.* **1997**, *119*, 9831.
(71) Smit, B. J.; Nguyen, M. T.; Bouma, W. J.; Radom, L. *J. Am. Chem. Soc.* **1991**, *113*, 6452.

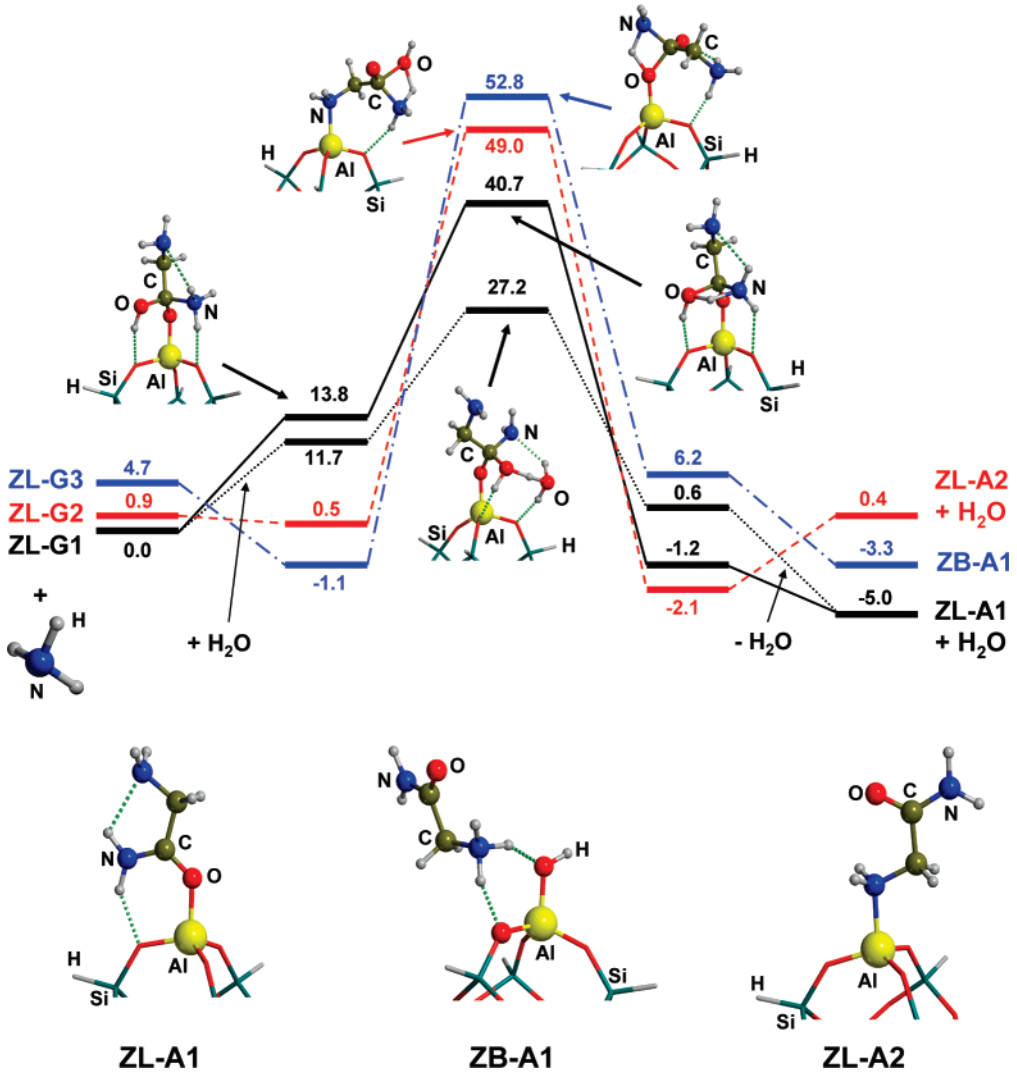

Figure 3. Relative free energy profiles (kcal mol^{-1}) for the concerted peptide bond formation processes on an isolated Lewis site taking the different isomers found as the reactive species: solid black lines refer to ZL−G1 prereactant complex; dash red lines refer to ZL−G2 prereactant complex; dash point blue lines refer to ZL−G3 prereactant complex; point black lines refer to ZL−G1 prereactant complex with an additional water molecule acting as proton solvent assistant. Relative free energies refer to ZL−G1 + NH_3 reference state. Bond distances are in angstroms.

water in proton transfer rate-determining steps, because it allows expansion of the nuclearity of the highly constrained fourth-membered ring, C−O···H···N, in the activated complex (see Figure 2 and Supporting Information for details). In principle, a similar lowering of the barriers should also be expected for the ZL−G2 and ZL−G3 cases. However, in those two cases, the extra hydrogen bonds between the water molecules and the rather basic oxygen atoms of the surface found in the ZL−G1 will be missing. In conclusion, the surface plays the role of enhancing the hydrogen bond strength within the ring where the proton transfer takes place for ZL−G1 only, so that the barrier lowering for Zl−G2 and ZL−G3, although expected, will be less dramatic.

The stepwise reaction has also been considered for the ZL−G1 case (available in Supporting Information), and the results obtained show that the barrier of the first (and highest step) is very close (40.8 kcal/mol) to that of the concerted reaction (40.7 kcal/mol) discussed above. Therefore, the surface Lewis sites of aluminosilicates catalyze the peptide bond formation indistinctly if it proceeds via either a concerted or stepwise mechanism.

Brønsted Site. Brønsted sites are usually well characterized in the interior of zeolites, and their acidic nature is due to the Si(OH)Al moiety, in which the proton compensates for the unbalanced charge due to the Si/Al substitution. To maximize the internal structural coherence between the cluster models mimicking Lewis and Brønsted sites, the very same cage cluster topology adopted for the Lewis site has been used to mimic the Brønsted as well. The Brønsted site is generated from the Lewis one by binding one proton of the Al-coordinated water to the nearby framework oxygen. The resulting structure, with the addition of one extra water molecule to simulate hydration, is shown in Figure 4.

In line with the Lewis case, the water displacement reaction by glycine was first analyzed and the optimized structures are shown in Figure 4, whereas the relative stabilities and reaction energies are given in Table 1, Brønsted section. Substitution of water by glycine is always favored, except for ZB−G3, which is about 8 kcal/mol less stable than the corresponding ZB−H_2O; the reason for that can be tracked by considering that water is a poorer proton donor than the COOH group of glycine (OH···OH 1.71 and 1.63 Å, for ZB−H_2O and ZB−G3, respectively)

Table 2. Activation Free Energies ($\Delta G^{\ddagger}$) and Free Reaction Energies (ΔG_r) of the Considered Processes[a]

	$\Delta G^{\ddagger}$	$\Delta G^{\ddagger}$ (G1)	ΔG_r	ΔG_r (G1)
gas phase				
$[G + NH_3 \rightarrow H_2NCH_2C(O)NH_2 + W]_c$	52.0		−1.1	
Lewis				
$ZL-G1 + NH_3 \rightarrow ZL-A1 + W$	40.7	40.7	−5.0	−5.0
$ZL-G2 + NH_3 \rightarrow ZL-A2 + W$	48.5	49.0	−0.5	+0.4
$ZL-G3 + NH_3 \rightarrow ZB-A1$	53.9	52.8	−8.1	−3.3
$[ZL-G1 + NH_3 + W \rightarrow ZL-A1 + 2\,W]_w$	27.2	27.2	−5.0	−5.0
$[ZL-G1 + NH_3 \rightarrow ZB-A2]_s$	40.8	40.8	+1.0	+1.0
Brønsted				
$ZB-G1 + NH_3 \rightarrow ZB-A1 + W$	49.0	49.0	−3.3	−3.3
$ZB-G2 + NH_3 \rightarrow ZB-A2 + W$	44.0	45.0	+0.1	+1.1
$ZB-G3 + NH_3 \rightarrow ZL-A1 + 2\,W$	8.2	17.9	−14.7	−5.0
Lewis/Brønsted				
$ZLB-G2 + NH_3 \rightarrow ZLB-A + W$	(22.1)	(26.2)	(−1.1)	(3.0)
	[11.6]	[15.5]	[−3.2]	[0.7]
$ZLB-G2 + G \rightarrow ZLB-GG + W$	(27.9)	(31.0)	(−2.6)	(1.5)
	[11.4]	[15.3]	[−9.0]	[−5.1]

[a] Subscripts C, W, and S refer to concerted, water-assisted, and stepwise mechanisms, respectively. $\Delta G^{\ddagger}$ and ΔG_r refer to the corresponding reaction, whereas $\Delta G^{\ddagger}$ (G1) and ΔG_r (G1) refer to the lowest energy asymptotes (i.e., $ZL-G1 + NH_3$, $ZB-G1 + NH_3$, and $ZLB-G1 + NH_3$ for Lewis, Brønsted, and Lewis/Brønsted-catalyzed reactions). Bare numbers at B1 = B3LYP/6-31+G(d,p), numbers in parentheses at B2 = B1//ONIOM[B3LYP/6-31+G(d,p):MNDO], and numbers in square brackets at B2+D (Grimme's dispersion[56] included). Data are in kilocalories per mole.

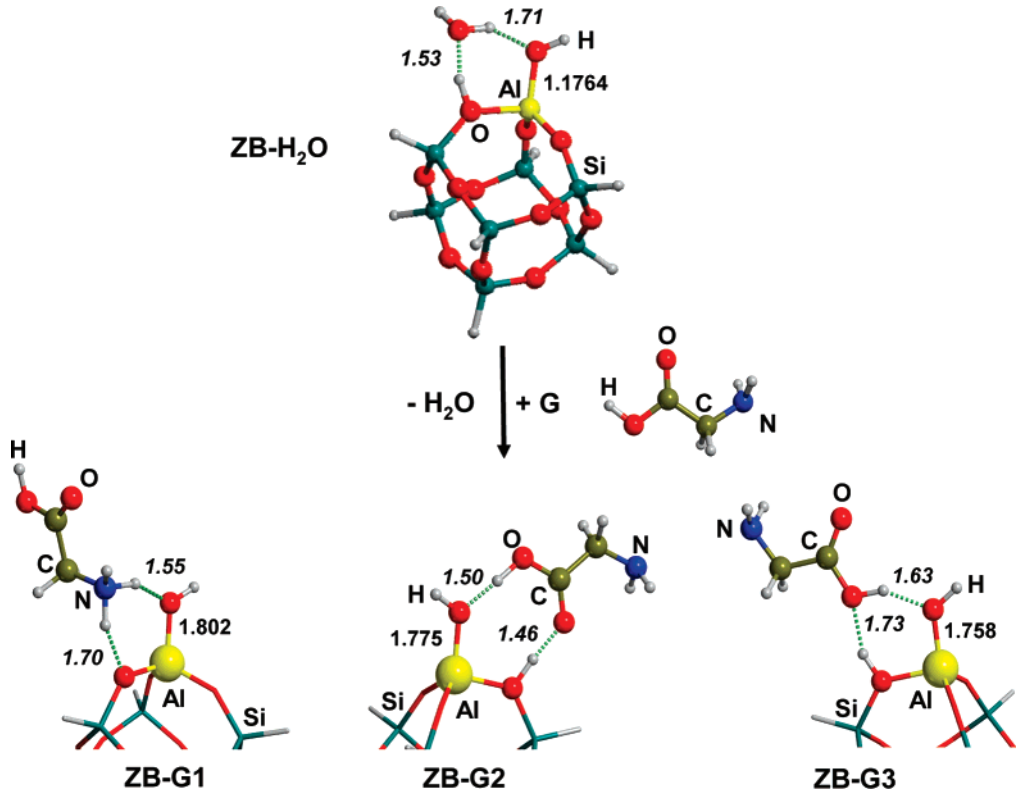

Figure 4. B3LYP/6-31+G(d,p)-optimized geometries of the cluster adopted to model the isolated Brønsted site interacting with water ($ZB-H_2O$) and of the structures found when adsorbed water is replaced by glycine (ZB−G1, ZB−G2, and ZB−G3). Bond distances are in angstroms.

but is, in turn, a better surface proton acceptor (H···O 1.53 and 1.73 Å, for $ZB-H_2O$ and ZB−G3, respectively). In the most stable adduct, ZB−G1, the adsorption of glycine is accompanied by a barrierless proton transfer from the surface Brønsted site to the NH_2 of glycine and the protonated $-NH_3^+$ group interacts with the negatively charged surface via two strong hydrogen bonds (Figure 4). This behavior was expected considering that ammonia (with a lower proton affinity than glycine) is usually protonated in acidic zeolites.[55,72−74] ZB−G2 structure shows two very short hydrogen bonds between the Brønsted acidic proton and the glycine C═O group on one side, and the carboxylic OH group and the surface terminal OH group on the other side.

The free energy profiles of the concerted reaction for the different isomers interacting with the Brønsted site, along with the most relevant structures, are shown in Figure 5. The reported energy values have been computed with respect to the $ZB-G1 + NH_3$ asymptote. Free energy barriers and free reaction energies are given in Table 2. Figure 5 shows that the free

(72) Brandle, M.; Sauer, J.; Dovesi, R.; Harrison, N. M. *J. Chem. Phys.* **1998**, *109*, 10379.

(73) Sauer, J.; Ugliengo, P.; Garrone, E.; Saunders, V. R. *Chem. Rev.* **1994**, *94*, 2095.

(74) Solans-Monfort, X.; Sodupe, M.; Mo, O.; Yanez, M.; Elguero, J. *J. Phys. Chem. B* **2005**, *109*, 19301.

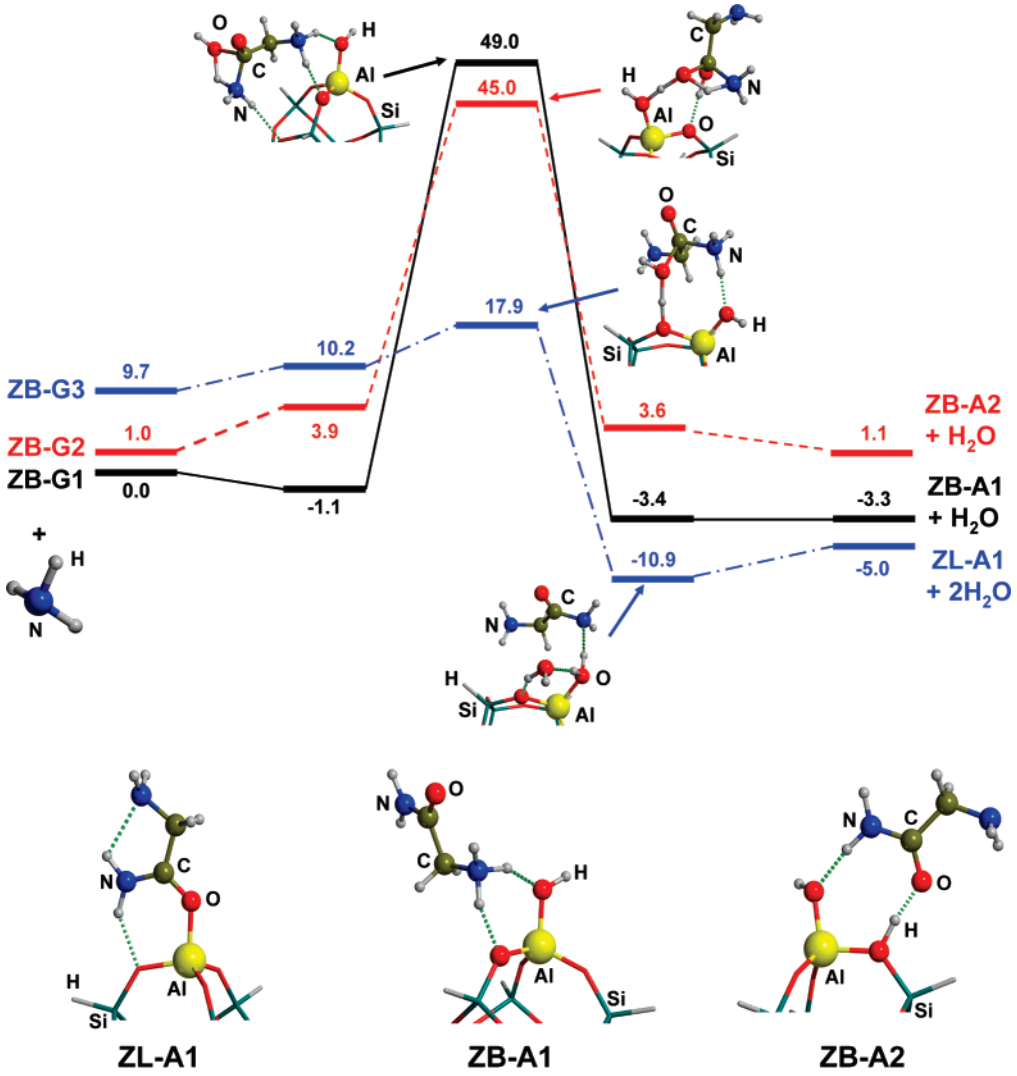

Figure 5. Relative free energy profiles (kcal mol^{-1}) for the concerted peptide bond formation process on an isolated Brønsted site taking the different isomers found as the reactive species: black solid lines refer to ZB−G1 prereactant complex; dash red lines refer to ZB−G2 prereactant complex; dash point blue lines refer to ZB−G3 prereactant complex. Relative free energies refer to ZB−G1 + NH_3 reference state. Bond distances are in angstroms.

activation energies for the two most stable adducts (ZB−G1 and ZB−G2) are relatively close to that of the uncatalyzed reaction. This means that neither the direct interaction of the carbonyl with the Brønsted site (ZB−G2) nor the protonation to the amino group (ZB−G1) will significantly enhance the electrophilicity of the CO group. Looking carefully at the two prereactant complexes for the ZB−G1 and ZB−G2 cases (Figure 5) reveals that the reason for the high barriers is the strained ring in which the proton transfer should take place and is similar to the cases described before for the Lewis activation. However, if one moves from the most stable prereactant complex (ZB−G1) to the least stable one (ZB−G3, about 10 kcal/mol higher in energy; Table 1), then a very favorable reaction path is found, the total energy barrier being only 18 kcal/mol (Table 2). The reason for such a dramatic barrier lowering is the presence of an eight-membered ring in which a double proton transfer occurs: one proton from the surface Brønsted site toward the glycine OH group and the other one from NH_3 to the surface aluminol group. Interestingly, the intermediate product envisages a Lewis site with two coordinated water molecules, one of them directly bounded to the Al atom and behaving as a strong Brønsted acid, as shown by the short hydrogen bond (H···N 1.83 Å; see Supporting Information) with the NH_2 group of the formed amide. The behavior of a water coordinated to a Lewis site showing strong Brønsted character has recently been proved by some of us.[75]

Lewis/Brønsted Interplay. The results obtained in the previously examined cases have to be considered with some caution, because (i) the Lewis and Brønsted sites are completely isolated from the mineral framework to which they belong and (ii) because of the relatively small size and topology of the adopted clusters, geometrical changes within the clusters during the reactions are relatively small. Point (ii) is important because the energetic cost of the geometrical reorganization of the active site during the catalytic process will increase the reaction barrier. For the above reasons, the free energy barriers obtained for the separated clusters (ZL and ZB) have to be considered as somehow underestimated. To overcome the above points, a larger and more realistic cluster has been cut out from the sanidine model of the feldspar surface (Figure 1), sporting both Lewis and Brønsted sites in close spatial proximity, so that an interplay between them in catalyzing the peptide bond formation

(75) Garrone, E.; Onida, B.; Bonelli, B.; Busco, C.; Ugliengo, P. *J. Phys. Chem. B* **2006**, *110*, 19087.

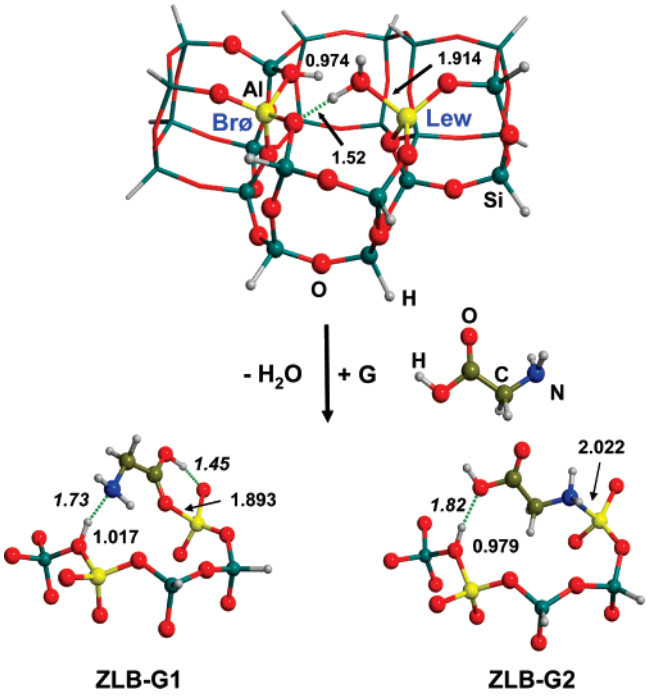

Figure 6. ONIOM2[B3LYP/6-31+G(d,p):MNDO]-optimized geometries of the cluster derived from the sanidine feldspar structure (Figure 1) to model the co-presence of Lewis and Brønsted sites on an aluminosilicate surface (ZLB−H_2O) and the structures in which glycine replaces the water adsorbed on the Lewis site (ZLB−G1, ZLB−G2). The region treated at high level of theory with the ONIOM2 method is shown as balls. For the sake of clarity, only a subportion of the high level zone is shown for ZLB−G1 and ZLB−G2 complexes. Distances are in angstroms.

should be expected (Figure 6). In virtue of the much stronger interaction energy of water on Lewis than on Brønsted sites (−20 and −6.3 kcal/mol for H_2O adsorbed on Lewis or Brønsted sites, respectively), only the former has been solvated by one water molecule. Because of the large size of the cluster model, calculations have been carried out using the ONIOM2 approach, described previously in the Computational Details. The ZLB−H_2O adduct shows that water bridges, via a rather short hydrogen bond, a second framework oxygen directly bound to the aluminum atom of the Brønsted site (Figure 6).

As done for the previous cases, the water displacement process by glycine has first been considered. ZLB−G1, the most stable complex (Table 1), envisages the glycine carbonyl oxygen bound to the surface Lewis site, the carboxylic proton making a hydrogen bond to a surface basic oxygen and the NH_2 group accepting a hydrogen bond from the surface Brønsted OH group (Figure 6, ZLB−G1). The ZLB−G2 structure is slightly more unstable than the ZLB−G1 one: the glycine NH_2 now bonds to the surface Lewis site and the OH group accepts a hydrogen bond from the surface Brønsted OH group. The Lewis/Brønsted section of Table 1 summarizes the reaction energies associated with the water displacement by the glycine ZLB−H_2O + G → ZLB−G + H_2O process and also the corresponding relative energies of the surface/adducts, at different levels of theory. For the ZLB cases, the B2 (B3LYP/6-31+G(d,p)//ONIOM2) energies are reported, because they are the closest to the full B3LYP/6-31+G(d,p) ones reported for the ZL and ZB separated clusters. Also, the correction of the DFT energy due to dispersive interactions has been estimated for the ZLB cluster only (see the Computational Details), and the corresponding values are reported in square brackets. As expected, the dispersive contribution is much more relevant for the ZLB−G adducts than for the ZLB−H_2O one because of the larger molecular size of glycine compared to water. The relative ZLB−G1/ZLB−G2 stability is, however, almost unchanged by the dispersive correction because of the close similarity of the two adducts (Table 1, numbers in square brackets). In principle, both ZLB−G1 and ZLB−G2 should undergo the reaction with NH_3 which mimics the second glycine needed for the peptide bond formation. However, previous results for the separated ZL and ZB cases (vide infra) showed that the Brønsted site was the most active catalyst (free barrier energy of about 18 kcal/mol; Table 2) when considering the ZB−G3 adduct as a starting configuration in which glycine is adsorbed through the Brønsted acidic site via its carboxylic group (Figures 4 and 5). For that reason and also to diminish the computational burden, ZLB−G2 has been selected as the best candidate for the peptide bond activation in virtue of its similarity with the ZB−G3 one (compare Figures 4 and 6, ZB−G3 and ZLB−G2, respectively). The relative ZLB−G2 population of $\sim 10^{-3}$ at equilibrium (computed using B2-D data of Table 1), compared with the most stable ZLB−G1 adduct, is high enough to provide a sufficient amount of ZLB−G2 on a geological time scale. Another reason to consider ZLB−G2 as the starting structure will also become clear in the next paragraph.

Figure 7a shows the energy profile for the reaction of NH_3 with the ZLB−G2 structure: the transition state activated complex reveals a structure that is very close to the one predicted for the smallest ZB cluster, whereas the final ZLB−A product remains attached to the mineral surface via a strong bond with the Lewis site and two hydrogen bonds with the regenerated Brønsted site (albeit with the acidic proton displaced on a different AlO_4 oxygen). At the bottom of Figure 7, the geometries of the two activated complexes (TS−Brø and TSLB1) are compared: for the more realistic ZLB cluster the acidic proton of the Brønsted site is more elongated than for the ZB case (1.27 vs 1.15 Å), whereas the hydrogen bond from the incoming NH_3 with the surface oxygen is shorter for the ZLB than for the ZB cluster (1.63 vs 1.68 Å). The new CN bond is shorter for the ZLB than for the ZB (1.54 vs 1.65 Å), and consequently the CO bond is longer for the former than for the latter (1.78 vs 1.66 Å), showing that the ZLB-activated complex resembles the final products more than the ZB one. All these effects reveal the higher acidic nature of the larger ZLB cluster than for the simplest ZB one. The B2 barrier with respect to the ZLB−G2 complex is only 22.1 kcal/mol (which becomes 26 kcal/mol when reference to the most stable ZLB−G1 complex is made; Table1), showing a relevant activation due to the mineral surface compared to the gas-phase reaction. The role of dispersion on the potential energy profile has also been studied: Figure 7a shows a dramatic reduction of the kinetic barrier, which is now as low as 12 kcal/mol with respect to the ZLB−G2 complex (16 kcal/mol with respect to the ZLB−G1 complex), resulting in a speeding up of the peptide bond formation of about 27 orders of magnitude compared to the gas-phase B1+D barrier of 47.8 kcal/mol. In the ZLB case, the dispersive correction is about 11 kcal/mol for the activated complex. The same B2+D calculation has also been carried out for the ZB-activated complex (derived from the ZB−G3 adduct; Figure 5), resulting in a reduction of the kinetic barrier by 7 kcal/mol, bringing the final barrier to 11 kcal/mol, very

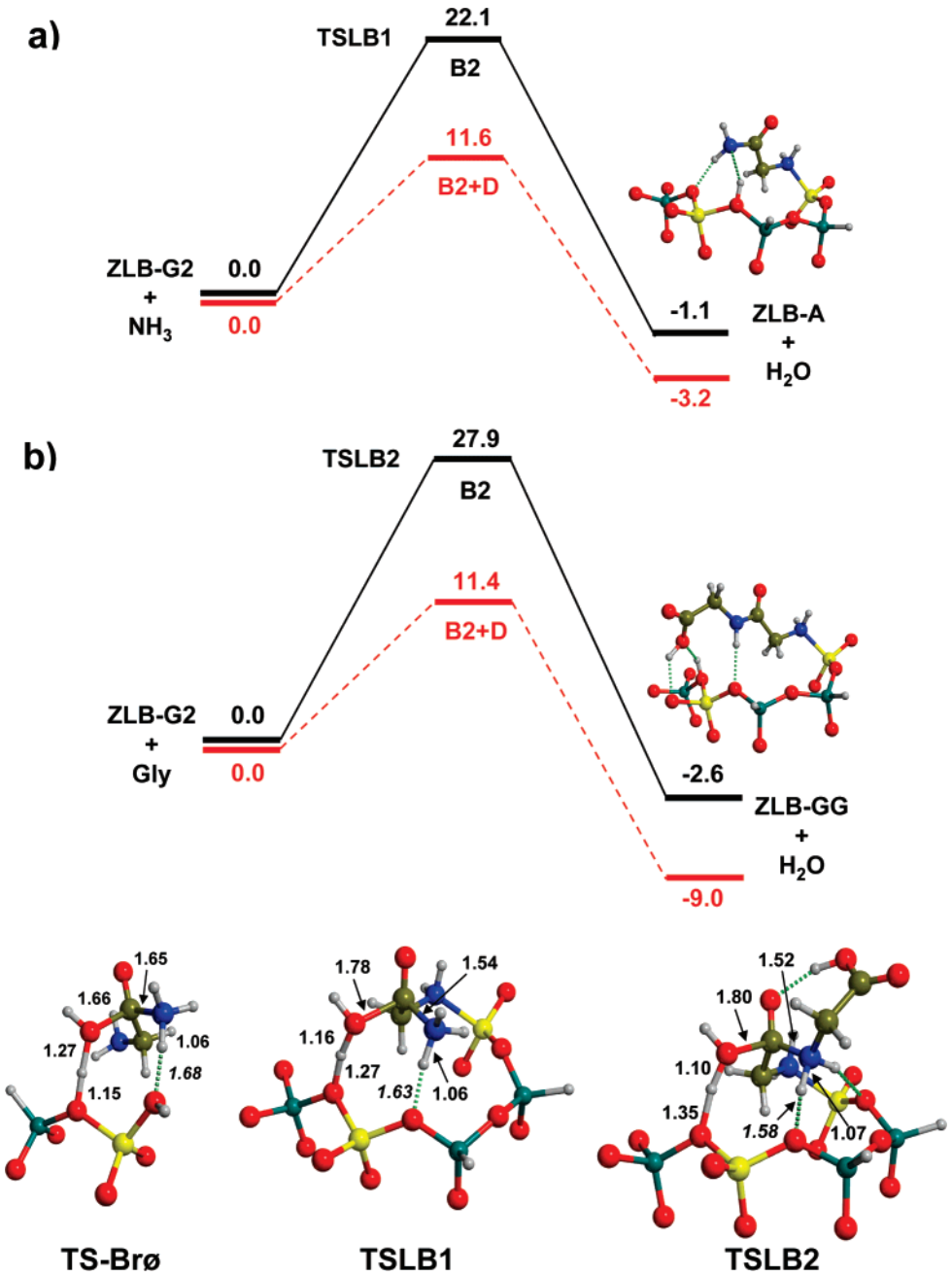

Figure 7. Free energy profiles (kcal mol^{-1}) of the peptide bond formation reaction taking ZLB−G2 as the prereactant complex. (a) Addition of NH_3. (b) Addition of glycine. Values reported in black are computed at the B2 = B3LYP/6-31+G(d,p)//ONIOM2[B3LYP/6-31+G(d,p):MNDO] level including the ONIOM2 thermal and entropic corrections. The free energy profiles reported in red (B2+D) include Grimme's dispersive correction[56] to the B2 free energies. Bottom: detailed view of the transition state-activated complexes for the isolated Brønsted (TS−Brø from the ZB−G3 complex) and for the Lewis/Brønsted (TSLB1 and TSLB2 for the addition of NH_3 and glycine, respectively) cases. Distances are in angstroms.

close to the value of 16 kcal/mol computed for the ZLB case using ZLB−G1 as a reference complex. It is reassuring that, despite the relatively large energetic cost of the geometrical reorganization for the ZLB cluster (computed to be 8.7 kcal/mol), the final barrier is close to that computed for the ZB model, in which this extra cost was negligible (computed to be 1.6 kcal/mol). Dispersive interactions are also important in stabilizing the final ZLB−A product: the B2 value of −1.1 kcal/mol becomes −3.2 kcal/mol when B2+D is adopted, as compared to the −1.7 kcal/mol value of the gas-phase process.

Encouraged by these results, we decided that the computational effort needed to study the reaction involving glycine molecule, rather than NH_3, was worth trying. Figure 7b shows the free energy profile resulting for the glycine addition to the ZLB−G2 adduct and the structure of the transition-state TSLB2. The B2 barrier associated with TSLB2 increases slightly to 28 kcal/mol because of higher entropic and deformation costs of glycine than NH_3. Dispersive contribution larger for glycine than for NH_3 dramatically decreases the barrier (data indicated as B2+D in Figure 7b) to 11.4 kcal/mol, close to that associated to the TSLB1 for the model reaction. However, it is worth noting the free energy of stabilization of the ZLB−GG product which is much larger than that computed for ZLB−A (Figure 7a). Dispersion correction higher for glycine than for NH_3 greatly stabilizes the newly formed dipeptide: −9.0 kcal/mol for ZLB−GG as compared with −3.2 for ZLB−A. From the kinetic point

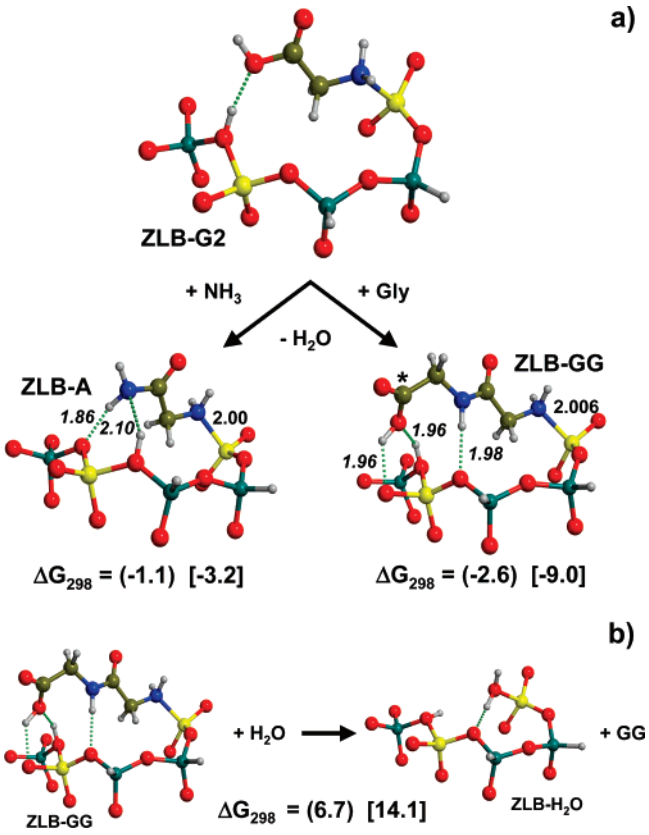

Figure 8. (a) Free energy of formation of ZLB−A and ZLB−GG products. The asterisk indicates the carbon atom at which the nucleophilic attack by an incoming glycine molecule will occur. (b) Water displacement process considering ZLB−GG as a reactant. Numbers in parentheses are B2 = B1//ONIOM[B3LYP/6-31+G(d,p):MNDO]; numbers in square brackets are B2+D (Grimme's dispersion[56] included). Data are in kilocalories per mole.

of view, the hydrolysis of ZLB−GG to give back the reactant ZLB−G2 and glycine is inhibited in comparison with the condensation process. The geometrical parameters of TSLB2 are close to those already described by TSLB1, although the former has a character closer to the product than the latter. In conclusion, the Brønsted/Lewis interplay allows first capturing glycine from the aqueous solution and securing it to the mineral surface via a strong interaction with the Lewis site via the NH_2 group, while the COOH moiety becomes activated toward nucleophilic attack by interacting with the nearby Brønsted site so that, when the reactions with NH_3 or glycine are considered, the kinetic barrier for the peptide bond formation is dramatically reduced and the product remains attached to the mineral surface because of the largest dispersive contribution of the surface compared to the gas-phase process.

From Dipeptides to Oligopeptides at the Aluminosilicate Surfaces. Results from the previous paragraph show that the ZLB−GG product will stay attached to the mineral surface and can also undergo a further nucleophilic attack by means of an incoming glycine molecule, at the carbon atom indicated by the asterisk in Figure 8a. This carbonylic carbon atom is activated toward nucleophilic attack so that the chain can be elongated, and if the surface presents enough acidic sites, this process can be iterated. To allow for the elongation process in a very dilute environment (as would probably be the case in the prebiotic world), the population of the ZLB−GG complex should be high enough to allow for numerous reactive encounters with glycine molecules in solution. Figure 8b shows the displacement reaction in which GG attached to the ZLB surface is exchanged by water: the reaction is strongly endergonic, the standard ΔG_{298} of reaction being 6.7 kcal/mol at the B2 level and 14.1 kcal/mol at the B2+D level. This means that the ZLB−GG product will stay available for a long time for further polymerization, even in the presence excess of water, in agreement with the suggestion put forward by Orgel[22] about polymerization on the rocks, in which the interaction of the polypeptide with the surface becomes more and more important as the chain lengthens due to favorable dispersive and electrostatic interaction with the mineral surface, allowing the possibility that the polypeptide coating of the surface will act as a further template.

Summary and Conclusions

Irrespective of the way in which important molecular building blocks were synthesized in the early days of the planet earth (within the first billion years), the problem of their polymerization resulting in the most relevant enzymes and nucleic acids is still an open question. An old but still fashionable proposal by Bernal[20] envisages a key role in the mineral surfaces, such as those of the clay family, which may have provided a way to concentrate the building blocks from the dilute primordial soup and also catalyze their polymerization by the active site present at their surfaces. Despite a great deal of successful experimental work (see Introduction) using silica, clays, alumina, and zeolites as minerals, very few attempts have been provided from the computational viewpoint to give a mechanistic interpretation of the catalytic role of those surfaces. The present article tries to fill in these gaps using clusters large enough to be representative of a true aluminosilicate surface and containing either independent Lewis or Brønsted as well as a Lewis/Brønsted pair. The B3LYP/6-31+G(d,p) free energy surfaces were fully characterized for the model reaction glycine + NH_3 → 2-NH_2 acetamide + H_2O (mimicking the full 2 Gly → GlyGly one), which is catalyzed by the described aluminosilicate clusters. The main conclusions can be drawn from comparing the B3LYP/6-31+G(d,p) activation energy of 50 kcal/mol for the uncatalyzed gas-phase reaction with that resulting from the catalyzed reactions. The high gas-phase energy barrier is due to the strained intramolecular proton transfer ring occurring at the transition structure. Using a simple cluster model for the Lewis site alone, we find that the barrier becomes 41 kcal/mol, whereas it decreases to 18 kcal/mol when the Brønsted site alone is involved. This dramatic reduction of the gas-phase energy barrier is achieved because the transition structure envisages a much less strained proton transfer ring in intimate contact with the surface atoms of the catalyst. For the very same reason, the barrier of 41 kcal/mol for the bare Lewis site was drastically reduced to 27 kcal/mol by the addition of one water molecule that acts as a proton transfer helper, which is further encouraged by the polarizing effect of the aluminosilicate surface oxygens in hydrogen bond contact with the extra water. Because the idea followed in this work was to consider, as a reference system, a sanidine feldspar surface rich in both Lewis and Brønsted sites in close spatial proximity, the interplay between both sites has also been studied using a larger and more representative cluster and the ONIOM2[B3LYP/6-31+G(d,p):MNDO] approximated method to save computer time. Furthermore, dispersive interactions, which were entirely missing with the B3LYP functional, have been computed by the Grimme[56] post-DFT correction and

proved to be very important for the largest cluster derived from the sanidine surface. Results show that, despite the much higher geometrical distortion cost during the process, the reaction occurring at the surface of the largest cluster sporting the co-presence of Lewis/Brønsted sites has the kinetic barrier for the peptide bond formation of only 16 kcal/mol (B2+D datum, ZLB−G1 as a reference complex), which causes a speeding up of 27 orders of magnitude compared to the reaction in gas phase. The lowering of the barrier has been achieved because the prereactant complex is firmly attached to the surface through the Lewis site, while the Brønsted site finally catalyzes the peptide bond formation. The product containing the newly formed peptide bond remains attached to the surface Lewis site and can be further attacked by another incoming glycine molecule to iteratively elongate its polypeptide chain. The formed product (envisaging the condensation of two glycine molecules) remains firmly attached to the surface, because exchange with the abundant water molecules is unfavorable ($\Delta G_{298} = 14.1$ kcal/mol at B2+D level). This means that the GlyGly adducts at the surface will survive long enough to further react with other incoming amino acid molecules, the adducts being activated toward nucleophilic attack because of the presence of neighboring surface Brønsted sites. While this may appear rather speculative, it is in agreement with a previous proposal[22] and opens the possibility that the inorganic surface will become coated by a polypeptide that may act as a biological template for subsequent synthesis of biologically relevant enzymes.

Acknowledgment. P.U. acknowledges the support of the HPC-Europa program, funded under the European Commision's Research Infrastructures Activity of the Structuring the European Research Area program, Contract No. RII3-CT-2003-506079, UAB (Contract No. VIS2005-17) for support, and the Generalitat de Catalunya Departament d'Educació i Universitats for a visiting professorship (Contract No. 2005PIV2-13). Financial support from the Italian Ministry MIUR (Project COFIN2004, Prot. 2004054901_003 coordinated by Prof. D. Ghigo) and by INSTM (progetto PRISMA 2002, coordinated by Professor C. Morterra: "Nanostructured oxidic materials for the adsorption and the catalysis") is gratefully acknowledged. Financial support from MCYT and DURSI, through the CTQ2005-08797-C02-02/BQU and SGR2005-00244 projects is gratefully acknowledged. A.R. is indebted to the UAB for a doctoral fellowship. CINECA and CESCA supercomputing centers are acknowledged for allowance of computer resources.

Supporting Information Available: Coordinates of all considered optimized structures along with absolute energies. Complete ref 50. This material is available free of charge via the Internet at http://pubs.acs.org.

JA070451K